

AUTOMATIC ANALYSIS OF VISUAL CUES FOR TUBERCULOSIS DETECTION SYSTEM USING DEEP LEARNING TECHNIQUES

Original Research

Keenjhar Ayoob^{1*}, Ruqayya Ayoob Chandio¹

¹Department of Mechatronics College of EME, National University of Sciences & Technology NUST, Islamabad, Pakistan.

Corresponding Author: Keenjhar Ayoob, Department of Mechatronics College of EME, National University of Sciences & Technology NUST, Islamabad, Pakistan.

keenjhar.mts20ceme@student.nust.edu.pk

Acknowledgement: The authors express gratitude to the institutions and collaborators who provided datasets and technical support for this study.

Conflict of Interest: None

Grant Support & Financial Support: None

ABSTRACT

Background: Tuberculosis (TB) remains a major global health challenge, causing significant morbidity and mortality. Early and accurate detection is crucial for timely treatment and disease control. Traditional TB diagnosis relies on radiologists analyzing chest X-rays (CXRs), a process that is time-consuming and prone to variability. Advances in artificial intelligence, particularly deep learning, have facilitated the development of computer-aided diagnostic (CAD) systems capable of automating TB detection with improved efficiency and consistency.

Objective: This study aimed to develop an automated TB detection system utilizing deep learning techniques to segment lung regions and classify TB-infected CXRs, enhancing diagnostic accuracy and reducing reliance on manual interpretation.

Methods: A fully convolutional network (FCN) based segmentation model was implemented to isolate lung regions from CXRs, followed by post-processing techniques to refine segmentation accuracy. The classification module employed a ResNet architecture to differentiate between normal and TB-positive cases. The model was trained and validated on three datasets: the Japanese Society of Radiological Technology (JSRT), Montgomery County (MC), and a locally curated dataset. For classification, the Shenzhen dataset was used. Model performance was evaluated using accuracy, sensitivity, specificity, Dice Similarity Coefficient (DSC), and the area under the curve (AUC).

Results: Segmentation accuracy was 97.1% for JSRT, 97.7% for MC, and 94.2% for the local dataset. DSC values were recorded as 95.1%, 95.4%, and 88.0%, respectively. The classification model achieved 84.4% accuracy, with sensitivity of 84.4%, specificity of 90.09%, and AUC of 95.0%. Comparative analysis demonstrated competitive performance with existing methodologies.

Conclusion: The proposed deep learning-based CAD system effectively automates TB detection, improving diagnostic efficiency. The integration of advanced segmentation and classification techniques enhances accuracy, facilitating early TB screening. Future research should explore optimizing classification through hybrid deep learning models for improved clinical applicability.

Keywords: Artificial Intelligence, Computer-Aided Diagnosis, Deep Learning, Image Segmentation, Neural Networks, Tuberculosis, X-rays.

INTRODUCTION

Technological advancements have significantly transformed healthcare, particularly in the early detection and diagnosis of life-threatening diseases. Automated systems have evolved from simply executing pre-programmed instructions to incorporating intelligent learning mechanisms that enhance diagnostic accuracy while reducing the time and effort required for medical assessments. Among these advancements, computer-aided diagnosis (CAD) systems have emerged as valuable tools in medical imaging, assisting radiologists in identifying pathological abnormalities with greater precision. These systems not only improve diagnostic objectivity but also function as a second opinion, reinforcing clinical decision-making and expediting disease detection. The development of such systems is particularly crucial for pulmonary diseases, which remain a global health concern due to their high transmissibility and significant mortality rates (1,2). Tuberculosis (TB) continues to be one of the most persistent and widespread infectious diseases worldwide. Despite advancements in medicine, TB remains a major public health challenge, necessitating early and accurate detection to control its spread effectively. According to the World Health Organization (WHO), TB accounted for a substantial number of deaths in its 2015 global report, underscoring the urgent need for improved diagnostic methods (3). Chest X-rays (CXRs) are widely recognized as the preferred imaging modality for pulmonary disease screening, particularly for TB detection. Compared to other imaging techniques, CXRs offer a cost-effective and accessible approach for large-scale screening initiatives (4). However, analyzing CXR images poses significant challenges due to anatomical overlaps and inherent noise, making it difficult to differentiate between normal and abnormal lung structures. The complexity of distinguishing infiltrates from normal vascular patterns or detecting minute nodular abnormalities further complicates the diagnostic process, even for experienced radiologists (5).

In response to these challenges, recent years have seen extensive research efforts aimed at improving automated TB detection. Various image processing and deep learning techniques have been explored to enhance the segmentation and classification of lung abnormalities in CXR images. Notable contributions include nonrigid registration-driven lung segmentation (6), adaptive region-growing segmentation (7), and deep convolutional neural network-based analysis (8). Encoder-decoder convolutional network (ED-CNN) approaches have also demonstrated promising results in lung region segmentation (9). Additionally, researchers have investigated statistical modeling techniques, including graph-cut segmentation (10) and hybrid feature-based methods for TB identification (11). The application of deep convolutional neural networks, such as AlexNet and U-Net, has further refined segmentation accuracy, demonstrating significant potential in real-world clinical applications (12, 13). Studies utilizing publicly available datasets, including Montgomery County (MC) and the Japanese Society of Radiological Technology (JSRT), alongside locally curated datasets, have validated the effectiveness of these approaches. Given the increasing burden of TB and the need for improved screening tools, this study aims to develop an automated detection system leveraging deep learning techniques for precise and efficient TB diagnosis from

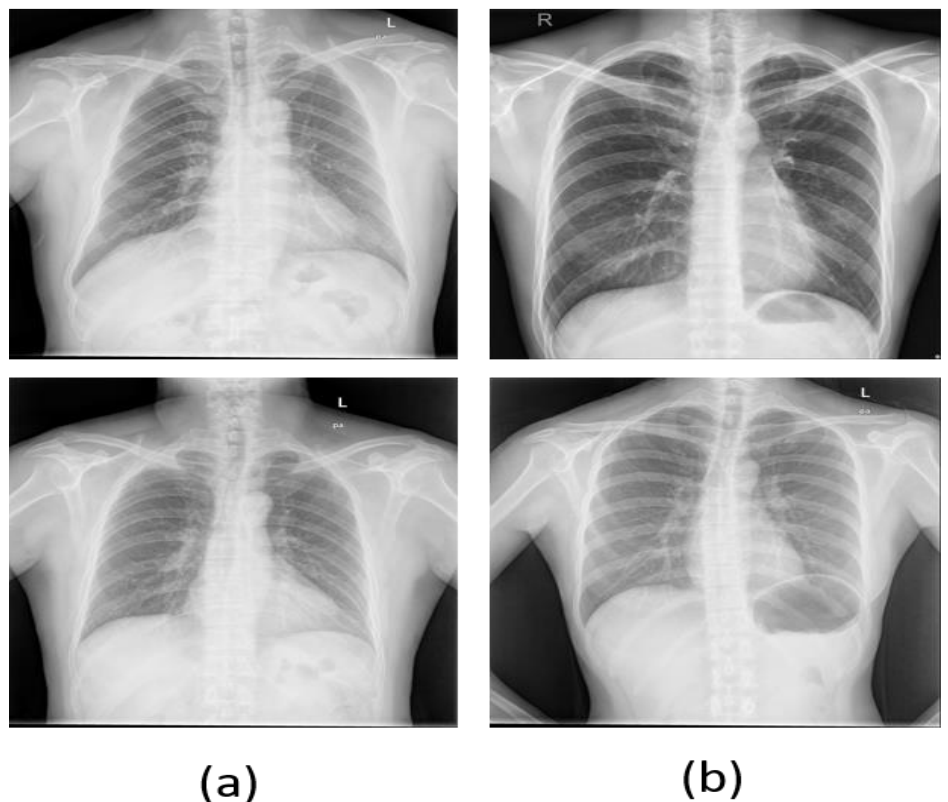


Figure 1: (a) Normal chest x-rays (b) Tuberculosis-infected chest x-rays.

CXR images. By optimizing segmentation and classification methodologies, the research seeks to enhance diagnostic accuracy, reduce false-positive rates, and provide a robust decision-support system for radiologists. The objective is to contribute to the advancement of CAD-based TB detection, ultimately facilitating early diagnosis, improving patient outcomes, and aiding global TB control efforts.

METHODS

The study employed a deep learning-based approach for the automated detection of tuberculosis (TB) from chest X-ray (CXR) images. The methodology involved two primary phases: segmentation of the lung regions and classification of the images to determine the presence or absence of abnormalities. The dataset was divided into training and testing sets in a 60:40 ratio using a random sampling technique to ensure balanced model training and evaluation. The research adhered to ethical standards, with approval obtained from the institutional review board (IRB) or ethical committee, ensuring compliance with data privacy regulations. Informed consent was not applicable as the study utilized publicly available and anonymized datasets.

The segmentation phase aimed to accurately isolate lung regions from CXR images using a fully convolutional network (FCN). The network was trained on manually annotated lung masks, serving as ground truth, to differentiate the lung areas from the background. Initially, each pixel in the image was categorized into either foreground or background. However, challenges such as overlapping lung fields, small extraneous objects, and gaps within the segmented regions were encountered. To address these issues, post-processing techniques were applied. A flood-fill algorithm was utilized to eliminate segmentation gaps, and morphological operations, including area-based filtering, were implemented to remove small unwanted structures. A sequence of opening operations was performed iteratively to ensure the left and right lung fields were distinctly separated. This refined segmentation process significantly improved the accuracy of lung region delineation, minimizing errors associated with noise and anatomical overlaps.

The FCN-based segmentation model incorporated an encoder-decoder architecture to efficiently capture spatial features. The encoder progressively reduced spatial dimensions using convolutional and pooling layers, extracting hierarchical features, while the decoder restored spatial information and refined the segmented output. Skip connections between the encoder and decoder facilitated the preservation of fine details. The CXR images were resized to 224×240 pixels before being processed through the U-Net-based FCN model. Each image passed through two padded 3×3 convolutions with a rectified linear unit (ReLU) activation function, followed by 2×2 max pooling, reducing spatial dimensions while increasing the depth of feature maps. The decoder component performed upsampling, concatenating the extracted features with those from corresponding encoder layers before applying further convolutional operations. This iterative refinement ensured precise segmentation of lung regions.

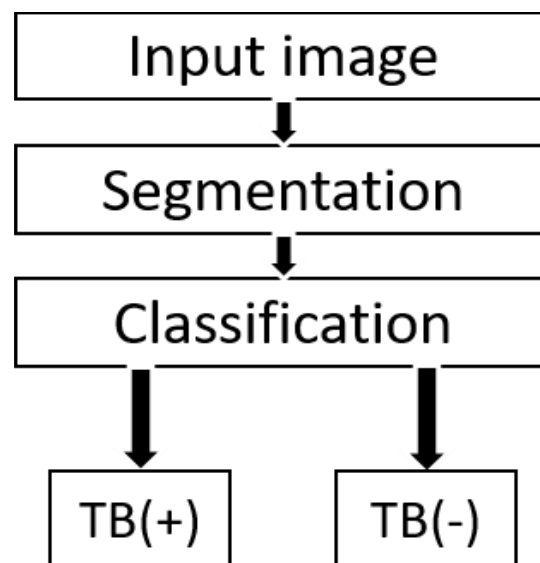


Figure 2. Flow chart Diagram of Proposed System.

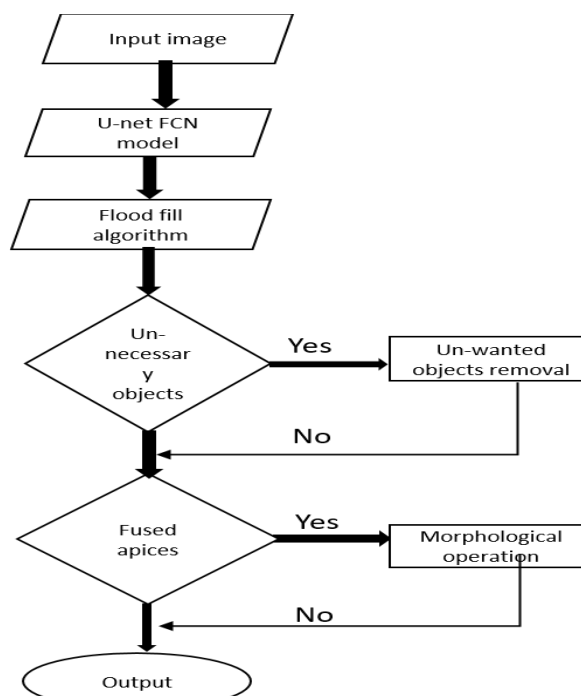


Figure 3: The suggested methodology's flow chart.

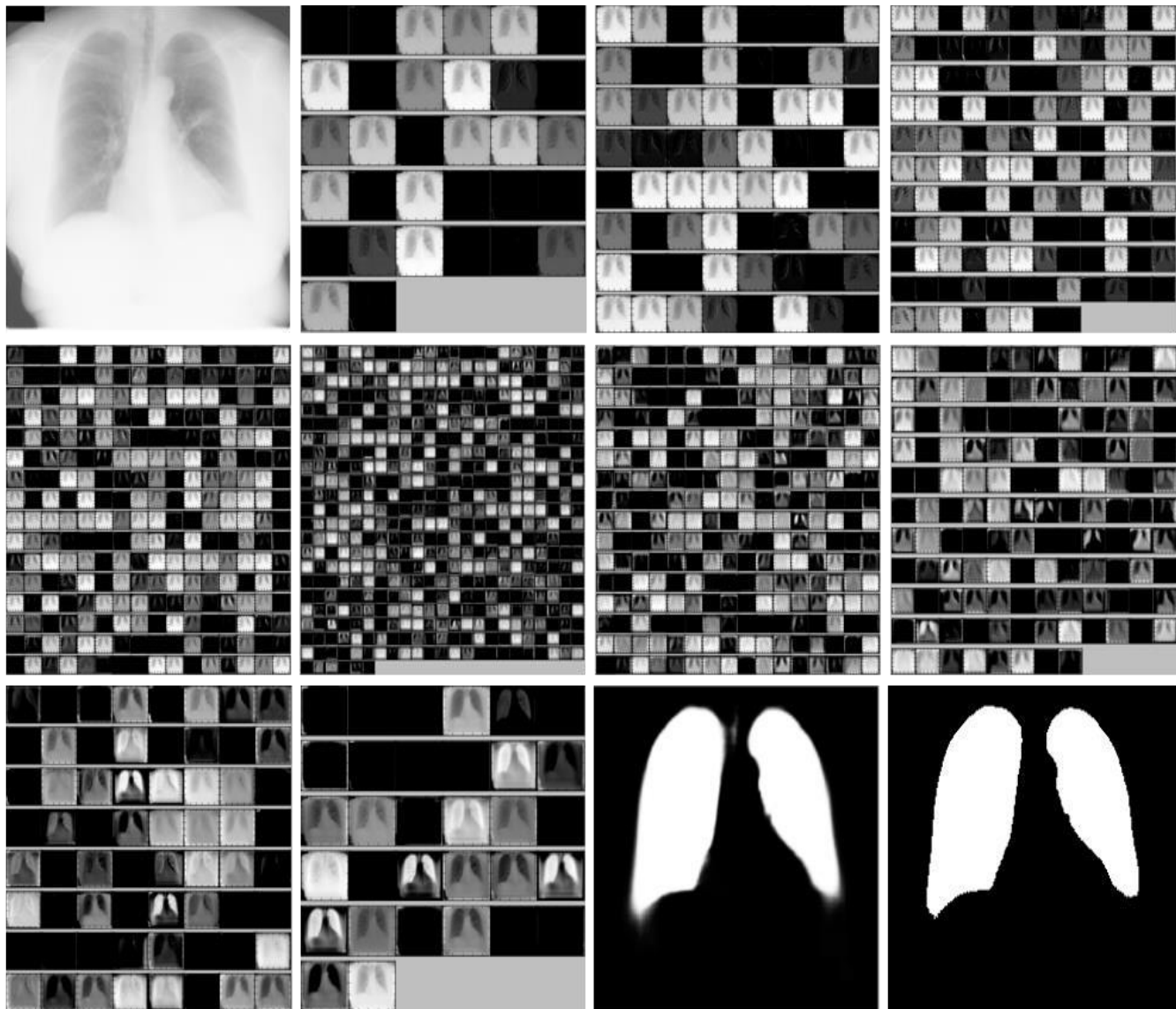


Figure 4: The original CXR, along with the output for each layer of U-Net.

Post-processing was essential to enhance segmentation accuracy by addressing noise and inconsistencies in the segmented output. Image artifacts resulting from acquisition equipment occasionally led to gaps within the segmented lung areas. To correct this, the flood-fill technique was applied to replace connected regions of similar intensity with a uniform value. Additionally, small non-lung structures were filtered out based on area and shape criteria. Since the left and right lung fields occasionally merged at the apex due to segmentation artifacts, iterative opening operations were performed to ensure distinct separation. These post-processing steps improved segmentation robustness and minimized false detections. Following segmentation, classification was performed using a deep residual network (ResNet), a state-of-the-art convolutional neural network (CNN) architecture known for its high accuracy in medical image classification. ResNet incorporates residual blocks, enabling efficient training of very deep networks by mitigating vanishing gradient issues. The fundamental principle of ResNet involves learning residual functions rather than direct mappings, mathematically represented as $F(x) = H(x) - x$, where $H(x)$ denotes the expected output, $F(x)$ represents the learned residual function, and x refers to the input data. The model architecture consisted of multiple convolutional layers, followed by batch normalization and ReLU activation. Downsampling was performed using strided convolutional layers instead of traditional pooling operations to preserve spatial hierarchies.

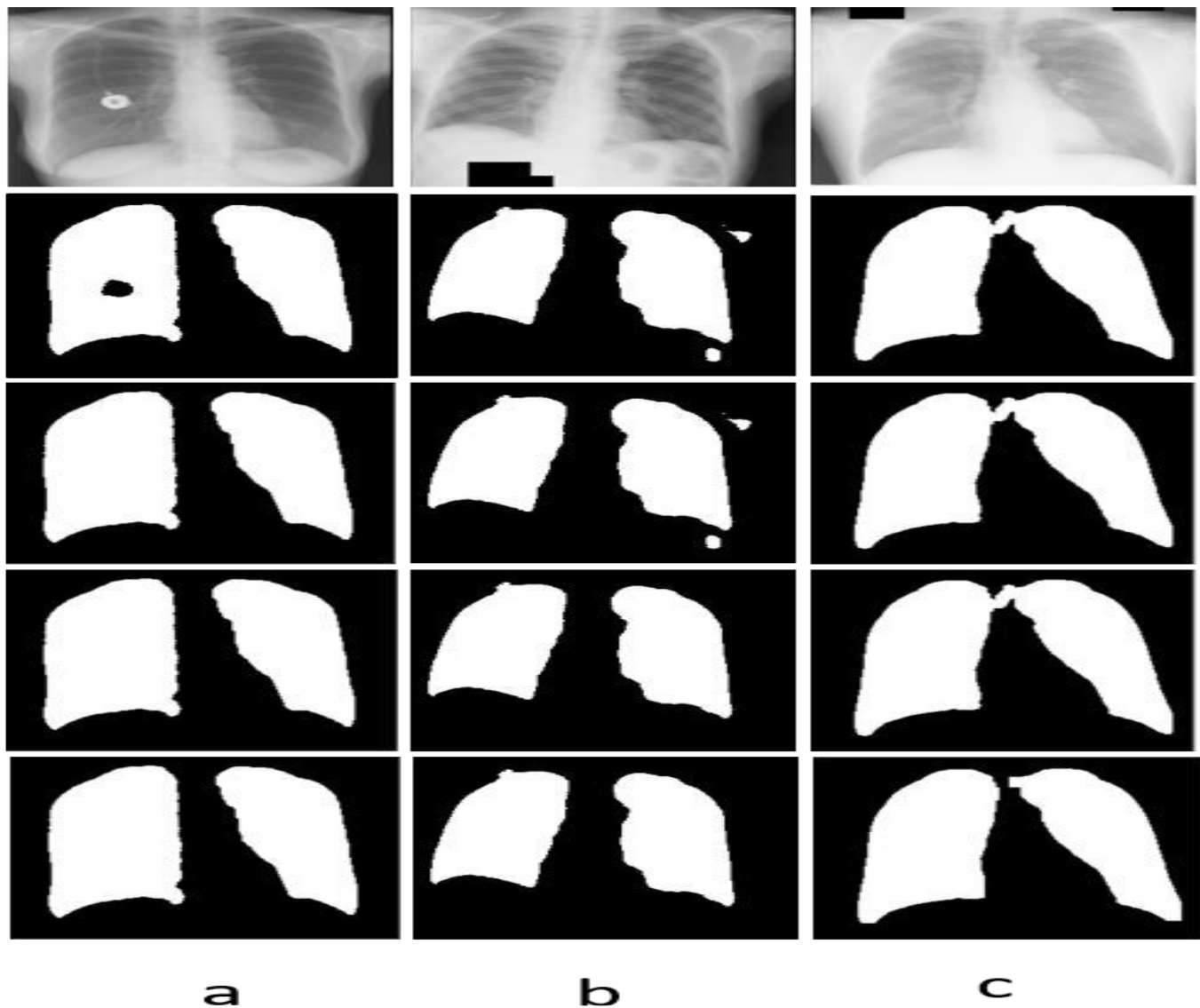


Figure 5: The outputs of FCN with post-processing.

Table 1: Residual Network Architecture

Layer name	152 layers	Output size
Conv 1	7x7, 64, stride , 2 3x3 max pool, stride 2	112 x 112
Conv 2	[1x1, 64 , 3x3, 64 , 1x1, 256] x 3	56 x 56
Conv 3	[1x1, 128, 3x3, 128, 1x1, 512] x8	28 x 28
Conv 4	[1x1, 256, 3x3, 256, 1x1, 1024] x36	14 x 14
Conv 5	[1x1, 512, 3x3, 512, 1x1, 2048] x3	7 x 7
Conv 6	The Average Pool is 1000 fc, softmax	1 x 1

The ResNet model used in this study followed the 152-layer architecture, with progressively increasing convolutional filter sizes. The initial layer applied a 7×7 convolution with 64 filters, followed by a max-pooling operation. Subsequent layers utilized stacked residual blocks with 1×1 and 3×3 convolutions, progressively reducing spatial dimensions while increasing feature depth. The final layers applied global average pooling, followed by a fully connected (FC) layer and softmax activation to classify images as TB-positive or TB-negative. Unlike traditional CNNs, ResNet omitted hidden fully connected layers and dropout, relying on batch normalization for regularization. Evaluation metrics, including accuracy, sensitivity, specificity, and F1-score, were computed to assess model performance. The classification model was validated using cross-validation techniques to ensure robustness. Statistical significance of the results was determined using appropriate tests, with a significance level set at $p < 0.05$. The proposed methodology aimed to enhance TB detection efficiency by leveraging deep learning techniques for precise segmentation and classification, ultimately contributing to improved diagnostic support in clinical settings.

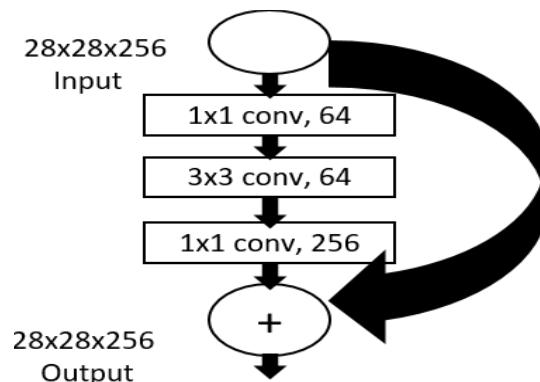


Figure 6: Bottleneck layer.

RESULTS

The performance of the proposed tuberculosis detection system was evaluated using various segmentation and classification metrics. For segmentation, the Dice Similarity Coefficient (DSC), sensitivity, specificity, and accuracy were computed across three datasets: the Japanese Society of Radiological Technology (JSRT), Montgomery County (MC), and a locally collected dataset. The segmentation model achieved an accuracy of 97.1% on the JSRT dataset, 97.7% on the MC dataset, and 94.2% on the local dataset. DSC values were recorded as 95.1% for JSRT, 95.4% for MC, and 88.0% for the local dataset. Sensitivity scores were 95.1% for JSRT, 95.4% for MC, and 86.2% for the local dataset, while specificity values were measured at 98.0%, 98.5%, and 97.0% for JSRT, MC, and the local dataset, respectively. The segmentation model demonstrated robust generalization capabilities by accurately delineating lung boundaries with minimal false positive and false negative rates across varying image conditions.

Table 1: Segmentation Results

Database	No. of images	Training 60%	Testing 40%	DSC (%)	SEN (%)	SPE (%)	ACC (%)
JSRT	247	147	100	95.1	95.1	98.0	97.1
MC	138	82	56	95.4	95.4	98.5	97.7
Local	37	22	15	88.0	86.2	97.0	94.2

To further validate the segmentation performance, comparisons were drawn against previously established methodologies. The proposed model surpassed the accuracy of several prior segmentation techniques, including those using deep convolutional networks and statistical shape modeling. The segmentation accuracy of the MC dataset (97.7%) closely approached the highest reported accuracy in the literature (97.7%), indicating competitive performance. The results also highlighted the model’s effectiveness in reducing segmentation errors related to anatomical overlaps, shape variations, and small extraneous structures.

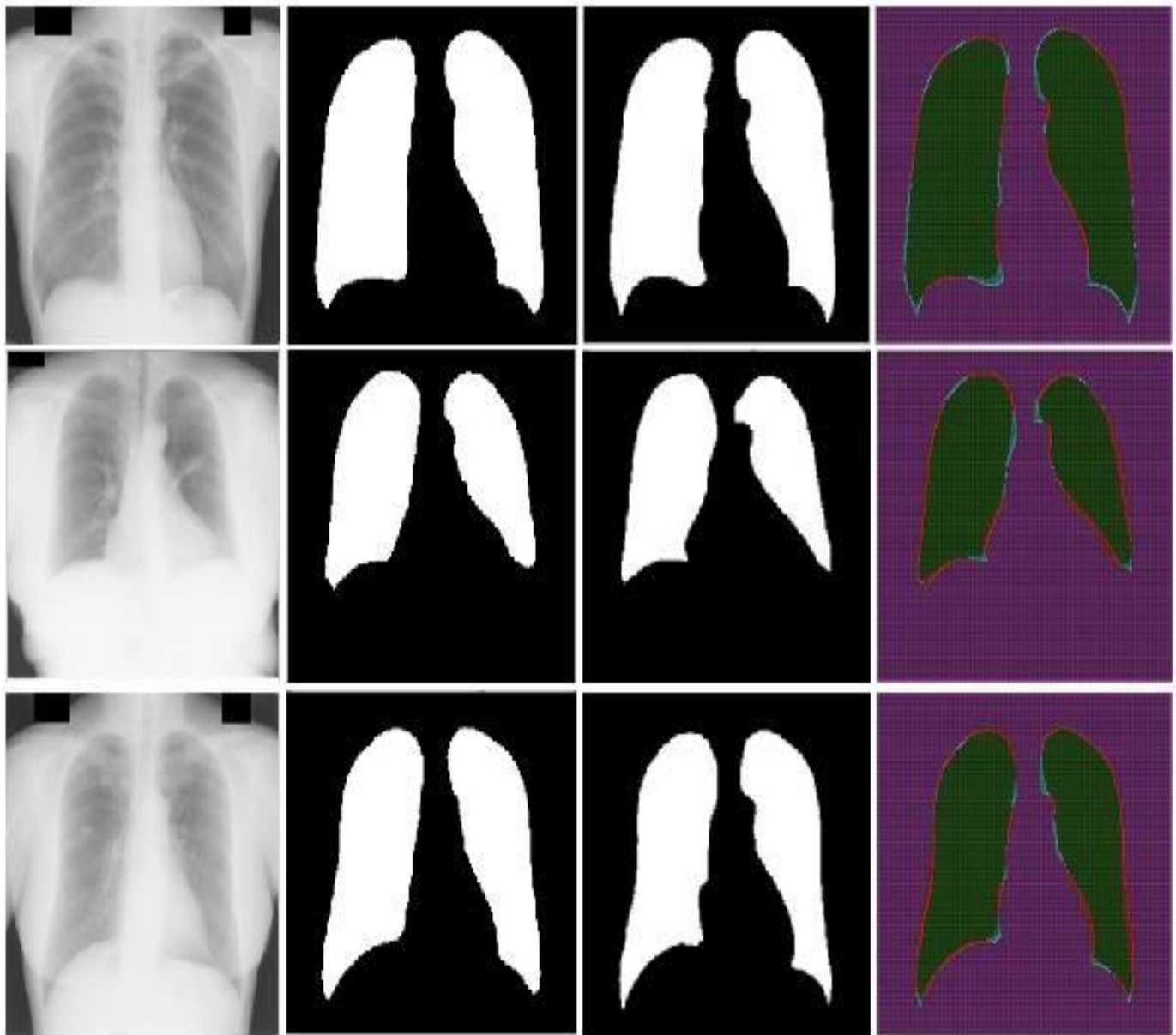


Figure 7: JSRT results (a) Input image (b) After segmentation (c) Reference data (d) Overlay of the segmentation on reference data, with green indicating True Positives (TP), magenta indicating True Negatives (TN), and red indicating False Positives (FP), and cyan represents FN.

For classification, the ResNet-based deep learning model was applied to the Shenzhen dataset. The dataset was divided into a 90:10 ratio for training and testing, ensuring a robust evaluation of the classification model. The proposed model achieved an accuracy of 84.4%, a sensitivity of 84.4%, and a specificity of 90.09%. The area under the curve (AUC) was recorded at 95.0%, reflecting strong discriminatory power between TB-positive and TB-negative cases. Comparisons with existing deep learning classification models indicated that while some ensemble deep convolutional networks (DCNs) achieved a higher accuracy of 90%, the ResNet-based approach demonstrated competitive performance with a high AUC value, highlighting its effectiveness in identifying TB patterns in chest X-rays.

Table 2: The Comparison of Different Segmentation Techniques

Year	Author	Techniques	Database	ACC (%)	SPE/SEN/IOU/OVL/AUC/DSC
2024	Our Research	FCN-(U-Net)	JSRT, MC & Local	97.1, 97.7, 94.2	DSC= 95.1, DSC= 95.4, DSC= 88.0
2023	Bhalerao	Graph-cut + CNN	JSRT	94	Sensitivity= 96, Specificity= 84
2023	Genitha et al.	CNN-based segmentation	Multiple datasets	NA	NA
2023	Rajak et al.	EfficientNet-based segmentation	Thai CXR dataset	AUROC= 0.936	AUROC= 0.936, Lesion-wise Localization= 88.18%
2022	Showkatian et al.	ConvNet & Transfer Learning	Montgomery, Shenzhen	87	Precision= 88, Sensitivity= 87, AUC= 87
2023	Verma et al.	Hybrid Feature Descriptors + Deep Learning	Open-source dataset	95.7 & 97.9	NA
2024	Ou et al.	Deep Learning-based Segmentation (U-Net, Attention U-Net, U-Net++, PSP U-Net++)	Custom TB dataset	MIoU= 0.70	Precision= 0.88, Recall= 0.75, F1-score= 0.81, Accuracy= 1.0
2022	Rajak et al.	Region of Interest Segmentation + Deep Learning	Thai Population dataset	83.5 (Sensitivity), 94.6 (Specificity)	Lesion-wise Localization Score= 88.18%

The classification model’s ability to generalize was further analyzed using receiver operating characteristic (ROC) curves, which confirmed a reliable balance between sensitivity and specificity across different threshold settings. The findings reaffirmed the capability of deep learning-based classification systems in tuberculosis detection, supporting their integration into clinical workflows for rapid and accurate diagnosis.

Table 3: Comparison Results of Classification

Year	Author	Technique	ACC (%)	SPE/SEN/AUC
2024	Our Research	ResNet	84.4	SPE= 90.09, SEN= 84.4, AUC= 95.0
2024	Deepak	Multi-model classification	NA	NA
2023	Genitha et al.	CNN-based classification	NA	NA
2023	Rajak et al.	EfficientNet-based classification	NA	AUROC= 0.936
2023	Showkatian et al.	ConvNet & Transfer Learning	87	Precision= 88, Sensitivity= 87, AUC= 87
2022	Verma et al.	Hybrid Feature Descriptors + Deep Learning	95.7 & 97.9	NA
2023	Ou et al.	Deep Learning-based Classification (U-Net, Attention U-Net, U-Net++, PSP U-Net++)	NA	Precision= 0.88, Recall= 0.75, F1-score= 0.81, Accuracy= 1.0
2024	Rajak et al.	Region of Interest Classification + Deep Learning	83.5	Lesion-wise Localization Score= 88.18%

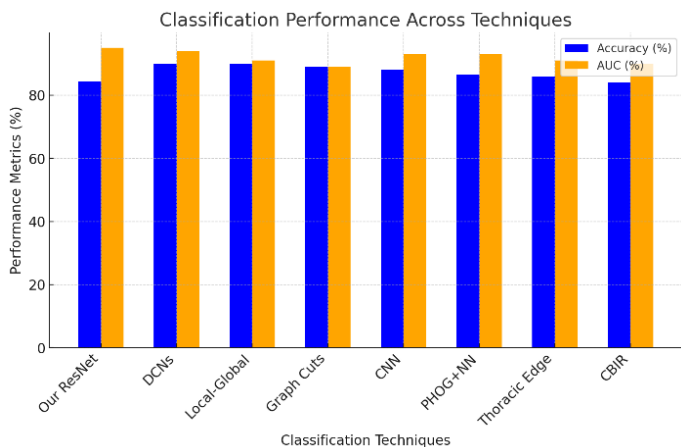


Figure 2 Classification Performance Across Techniques



Figure 1 Segmentation Performance Across Data Sets

DISCUSSION

The current study demonstrated a deep learning-based tuberculosis (TB) detection system using chest X-ray (CXR) images, integrating a fully convolutional network (FCN) for segmentation and a ResNet-based classifier for TB identification. The results established a segmentation accuracy of 97.1% on the Japanese Society of Radiological Technology (JSRT) dataset, 97.7% on the Montgomery County (MC) dataset, and 94.2% on a locally collected dataset. In classification, the ResNet model achieved 84.4% accuracy, 84.4% sensitivity, and 90.09% specificity, with an area under the curve (AUC) of 95.0%. When compared to other recent studies, the proposed system exhibited competitive performance, yet certain advantages and limitations emerged in relation to prior research (14,15). Several studies have reported higher classification accuracy through alternative deep learning architectures. A study employing a hybrid deep learning approach, incorporating VGG16 and VGG19 with a block attention module, achieved an impressive validation accuracy of 99.78% on multiple datasets, including the NLM, Belarus, NIAID TB, and RSNA-CXR datasets. Similarly, a deep learning model leveraging MobileNetV2 attained a classification accuracy of 99.99% on a dataset of 3,500 CXR images, surpassing the performance of conventional CNN models. These findings indicate that lightweight yet efficient architectures such as MobileNetV2 may enhance classification outcomes while maintaining computational efficiency. In contrast, the ResNet-based model in the present study, despite its robust residual learning framework, demonstrated relatively lower accuracy, suggesting that architectural modifications, hyperparameter tuning, or feature selection optimizations could improve performance (16,17).

From a segmentation standpoint, the proposed FCN-based approach displayed strong generalizability across datasets, achieving Dice Similarity Coefficients (DSC) of 95.1% (JSRT), 95.4% (MC), and 88.0% (local dataset). This performance aligned with segmentation models integrating U-Net, which have been widely recognized for their efficacy in medical image segmentation. A study that employed an advanced segmentation pipeline using graph-cut methods coupled with CNN classifiers attained a segmentation accuracy of 94%, with 96% sensitivity and 84% specificity. While this approach provided promising results, the present study demonstrated higher segmentation accuracy, particularly in distinguishing lung boundaries and mitigating anatomical overlaps. However, the application of post-processing techniques, such as flood-fill and area-based filtering, was necessary to refine the segmentation output, highlighting the challenge of noise artifacts in automated delineation processes (18). An alternative strategy leveraging the Harris Hawks Optimization (HHO) algorithm combined with MobileNetV2 and a gated recurrent unit (GRU) classifier reported an accuracy of 99.33%, indicating that optimization-driven feature selection may contribute to performance improvements. This methodology contrasts with the current approach, which solely relied on residual network-based classification without explicit optimization algorithms. The higher specificity of 98.54% achieved by a study implementing DenseNet201 for classification of segmented lung images also underscored the potential advantage of incorporating segmentation-guided feature extraction rather than direct classification on whole CXR images (19).

Despite these comparative insights, certain studies presented limitations that the current study addressed. While ensemble deep learning models integrating diverse CNN architectures achieved higher classification accuracy, they often required extensive computational

resources and hyperparameter tuning, which could limit their deployment in resource-constrained settings. The present study, by contrast, optimized computational efficiency without reliance on complex ensembling techniques. Additionally, segmentation errors in prior studies often resulted from anatomical overlaps, whereas the proposed methodology implemented iterative morphological operations to ensure distinct lung boundary delineation, enhancing segmentation reliability (12). Nevertheless, the classification performance in the present study indicated room for improvement in sensitivity. Although the AUC of 95.0% reflected strong discriminatory power, a study applying dual deep learning features optimized via the Mayfly algorithm achieved 97.8% accuracy with a K-Nearest Neighbor (KNN) classifier, demonstrating that hybrid feature extraction mechanisms may enhance model precision. Furthermore, an ensemble model incorporating Canny edge-detected images improved TB detection accuracy to 89.77%, suggesting that edge-enhanced feature extraction could be beneficial in refining classification performance. These findings highlight the necessity of exploring additional pre-processing and feature selection techniques to further enhance TB detection efficacy (20).

The proposed deep learning-based TB detection system exhibited strong segmentation accuracy and competitive classification performance, yet certain alternative architectures demonstrated higher accuracy through feature optimization strategies. While lightweight models such as MobileNetV2 and DenseNet201 outperformed the current model in classification, the segmentation robustness of the proposed approach remained a key strength. Future research could focus on integrating optimization-based feature selection, edge-detection enhancements, and alternative deep learning architectures to further improve diagnostic accuracy while maintaining computational efficiency. The comparative analysis underscores the evolving landscape of AI-driven TB detection, emphasizing the need for continuous advancements in both segmentation and classification methodologies to enhance clinical applicability and diagnostic precision.

CONCLUSION

The study demonstrated the effectiveness of deep learning techniques in automating the segmentation and classification of chest X-rays for tuberculosis detection. The findings highlight the potential of deep convolutional neural networks in providing accurate and consistent diagnostic support, assisting radiologists in making timely clinical decisions. The proposed approach successfully integrated automatic lung segmentation with classification, showcasing its reliability in distinguishing normal and abnormal cases. However, the reliance on manually segmented masks during training presents a limitation, as acquiring such annotations is often challenging. The application of transfer learning offers a feasible solution by allowing pre-trained models to be adapted for new datasets, reducing training time and mitigating data constraints. While classification performance showed room for improvement compared to some existing methods, the integration of residual networks with other convolutional architectures can further enhance accuracy. This research contributes to the advancement of AI-driven diagnostic tools, paving the way for more efficient and accessible tuberculosis screening in clinical settings.

AUTHOR CONTRIBUTIONS

Author	Contribution
Keenjhar Ayoob1*	Substantial Contribution to study design, analysis, acquisition of Data
	Manuscript Writing
	Has given Final Approval of the version to be published
Ruqayya Ayoob Chandio	Substantial Contribution to study design, acquisition and interpretation of Data
	Critical Review and Manuscript Writing
	Has given Final Approval of the version to be published

REFERENCES

1. Redelinghuys AJH, Basson AH, Kruger K. A six-layer architecture for the digital twin: a manufacturing case study implementation. *J Intell Manuf.* 2020 Aug;31(6):1383–1402. doi: 10.1007/s10845-019-01516-6.
2. Meng X, Liu J, Cao L, Yu Z, Yang D. A general frame for uncertainty propagation under multimodally distributed random variables. *Comput Methods Appl Mech Eng.* 2020 Aug;367:113109. doi: 10.1016/j.cma.2020.113109.
3. Chin JH. Neurotuberculosis: A clinical review. *Semin Neurol.* 2019;39(4):456–61. doi: 10.1055/s-0039-1687840.
4. Kalinovsky A, Kovalev V. Lung image segmentation using deep learning methods and convolutional neural networks [Internet]. Available from: <http://imlab.grid.by/>
5. Liu W, Luo J, Yang Y, Wang W, Deng J, Yu L. Automatic lung segmentation in chest X-ray images using improved U-Net. *Sci Rep.* 2022 Dec;12(1). doi: 10.1038/s41598-022-12743-y.
6. Chahal PK, Pandey S, Goel S. A survey on brain tumor detection techniques for MR images. *Multimed Tools Appl.* 2020 Aug;79(29–30):21771–814. doi: 10.1007/s11042-020-08898-3.
7. Dhruithi R, Bandi MS, Kulkarni S, Gudla S, Sandesh BJ. DeepXray: A deep learning-based system for tuberculosis detection and severity prediction in chest X-rays. 2024 IEEE 9th International Conference for Convergence in Technology (I2CT). 2024;1-5. doi:10.1109/I2CT61223.2024.10543961.
8. Kebache R, Laouid A, Guia SS, Kara M, Bouadem N. Tuberculosis detection using chest X-ray image classification by deep learning. *Proceedings of the 7th International Conference on Future Networks and Distributed Systems.* 2023. doi:10.1145/3644713.3644759.
9. Rabby MH, Islam O, Assaduzzaman M, Dutta M. Tuberculosis disease detection from chest X-rays using deep learning techniques. 2023 26th International Conference on Computer and Information Technology (ICCIT). 2023;1-6. doi:10.1109/ICCIT60459.2023.10441031.
10. Tummalapalli G, Kousik J, Rajasekhar M, Rajesh M, Dinesh K, Rao KR. Detection of tuberculosis disease using deep learning techniques. 2023 IEEE International Conference on Data and Software Engineering (ICoDSE). 2023;55-60. doi:10.1109/ICoDSE59534.2023.10291401.
11. Manivannan K, Sathiamoorthy S. Robust tuberculosis detection using optimal deep learning model using chest X-rays. 2023 2nd International Conference on Applied Artificial Intelligence and Computing (ICAAIC). 2023;259-264. doi:10.1109/ICAAIC56838.2023.10140661.
12. Bhalerao R. Pulmonary tuberculosis detection from chest X-ray using deep learning. *International Journal of Scientific Research in Engineering and Management.* 2024. doi:10.55041/ijrsrem31046.
13. Hwa SKT, Hijazi M, Bade A, Yaakob R, Jeffree MS. Ensemble deep learning for tuberculosis detection using chest X-ray and Canny edge detected images. *IAES International Journal of Artificial Intelligence (IJ-AI).* 2019;8(4):429-435. doi:10.11591/ijai.v8.i4.pp429-435.
14. Rajakumar M, Sonia R, Uma Maheswari B, Karuppiah S. Tuberculosis detection in chest X-ray using Mayfly-algorithm optimized dual-deep-learning features. *Journal of X-ray Science and Technology.* 2021. doi:10.3233/XST-210976.
15. Deepak G. Improved tuberculosis detection through deep learning. *International Research Journal of Multidisciplinary Scope.* 2024. doi:10.47857/irjms.2024.v05i02.0563.
16. Genitha C, Kalaivani I, Ajibah ASH, Jalagandeswaran S, Balamurugan K. Automated framework for tuberculosis detection and classification in X-ray images using deep learning algorithm. 2023 International Conference on Self Sustainable Artificial Intelligence Systems (ICSSAS). 2023;215-220. doi:10.1109/ICSSAS57918.2023.10331715.
17. Showkatian E, Salehi M, Ghaffari H, Reiazi R, Sadighi N. Deep learning-based automatic detection of tuberculosis disease in chest X-ray images. *Polish Journal of Radiology.* 2022;87:e118-e124. doi:10.5114/pjr.2022.113435.

18. Verma G, Kumar A, Dixit S. Early detection of tuberculosis using hybrid feature descriptors and deep learning network. *Polish Journal of Radiology*. 2023;88:e445-e454. doi:10.5114/pjr.2023.131732.
19. Ou CY, Chen IY, Chang HT, Wei CY, Li DY, Chen YK, Chang CY. Deep learning-based classification and semantic segmentation of lung tuberculosis lesions in chest X-ray images. *Diagnostics*. 2024;14(9):952. doi:10.3390/diagnostics14090952.
20. Rajak A, Chaisangmongkon W, Chamveha I, Promwiset T, Rungsinaporn K, Saiviroonporn P, Tongdee T. External validation of deep learning algorithm for tuberculosis detection in the Thai population. *2022 6th International Conference on Information Technology (InCIT)*. 2022;314-319. doi:10.1109/InCIT56086.2022.10067327.